IOP Conf. Series: Earth and Environmental Science **161** (2018) 012005 doi:10.1088/1755-1315/161/1/012005

Daily direct, diffuse and global irradiances modelling for an accurate estimate of daily solar radiation intensity at the city of El Jadida (Morocco)

M Zaimi, H El Achouby, A Ibral and E M Assaid
Optics and Electronics of Semiconductor Nanostructures Team, Laboratory of Instrumentation, Measurements and Control, Department of Physics, Faculty of Sciences, Chouaib Doukkali University, P. O. Box 20 El Jadida, Morocco
E-mail:eassaid@yahoo.fr

Abstract. In this work, we derive analytic expressions and calculate numerical values of incident daily solar radiation on horizontal, fixed tilted, single-axis and double-axis tracking apertures as functions of day number, collector latitude, tilt and azimuth angles. The effect of non-uniform atmospheric absorption of incident radiation throughout a day is taken into account and new models of direct normal B_n and diffuse horizontal D_h components of global horizontal (tilted) irradiance G_h (G_t) are proposed, tested and validated on local experimental measurements. This enables us to extract global irradiance model parameters for average day of each month and to predict, accurately, daily solar radiation (energy per unit area) effectively received by any collector placed on earth during the whole year.

1. Introduction

Today, global energy demand is increasing exponentially. This is mainly due to increase of energy needs of newly industrialized or emerging countries such as China, India, Brazil, Indonesia, Mexico, South Africa or Turkey [1]. Meanwhile, major oil and natural gas discoveries throughout the world are scarce and world fossil energy reserves increase slightly. In addition, excessive consumption of coal and fossil fuels increases carbon levels in the atmosphere and generates air pollution and climate perturbation resulting in floods followed by long periods of drought [2]. The inadequacy between increase in demand and that in energy reserves as well as the climate change and its disastrous consequences has impelled political and economic decision-makers to turn to renewable energy sources which are more abundant and more respectful for environment. Solar energy, with its two components: Concentrated Solar Power (CSP) and Photovoltaic (PV), is the flagship renewable energy, it is at the center of interest of any government that seeks to diversify its bouquet of energy. The government of Morocco has established an energy plan aiming to reduce carbon footprint of the country and to increase the share of renewable energies to 42% of the global capacity by 2020 before to achieve 52% share of renewable energies by 2030 [3-5]. The high point of this plan was the inauguration, in February 2016, of the first part of solar power plant Noor Ouarzazate (NOORo I) [6]. NOORo I uses solar thermal technology with parabolic cylindrical troughs to capture sunlight. By 2020, NOORo I, II, III and IV will be able to generate 580 MW of electric power. They will also allow an annual saving of greenhouse effect gases equivalent to 3.7 million tones of CO_2.

Before opting for such technology, a preliminary study of incident solar radiation throughout the year as well as the knowledge of number of sunny days per year are required. In the present work, we will attempt to address these two issues. More precisely, we will investigate the solar potential in the city of El Jadida (33° 15’ 00’’ N, 8° 30’ 00’’ W) which is situated on Moroccan Atlantic coast. To our knowledge, there is only one complete study which was devoted to characterization of solar potential at the site of El Jadida [7]. In this thesis, the author measured hourly, daily, monthly and yearly direct, diffuse and global solar irradiance falling on a horizontal collector during two years. In the present paper we will give analytical models of daily diffuse, direct and global irradiance and proceed to extraction of model parameters. We use this models to predict energy densities received by horizontal and fixed tilted

collectors during a given day. We compare these densities to local experimental values. The present paper may be broken into five sections. In the second section, physics and astronomy backgrounds necessary for the calculation of incident irradiance (energy density per unit of time and area) on a given aperture at higher atmosphere boundary are presented. In the third section, details of calculations of daily solar radiation (energy density per unit area) radiated on horizontal, fixed tilted, double-axis tracking, north to south oriented single-axis tracking and east to west oriented single-axis tracking apertures placed at higher atmosphere border are presented. In the fourth section, effects of non-uniform atmospheric absorption throughout a day are taken into account and models of direct normal B_n and diffuse horizontal D_h components of daily global horizontal (tilted) irradiance G_h (G_t) are proposed, tested and validated using local irradiance experimental data. Then, the extracted model physical parameters are used to accurately predict, the daily solar energy per unit area (radiation) effectively received by all types of collectors placed on earth for each day of the year. A comparison between measured and predicted daily global horizontal irradiances over one year is done and acceptable agreement is found.

2. Physics background and theoretical framework

2.1. The non-uniform extra-atmospheric spectral irradiance

The spectral irradiance is the power per unit area in a very short spectral range $d\lambda$, its unit is $\mathrm{Wm^{-2}\mu m^{-1}}$. Considering isotropic solar emission, the non-uniform extra-atmospheric spectral irradiance received by a point at the top of terrestrial atmosphere is [8]:

$$I_\lambda = S_{sun}\left(E_\lambda \Big/ \int_0^\infty E_\lambda d\lambda\right) \tag{1}$$

S_{sun} is the solar ‘‘constant’’ [8], it represents the total power per unit area radiated to a square meter of an extra-atmospheric surface normal to the sun’s rays and placed at a distance equal to one astronomical unit $\left(1\mathrm{AU} = 1.496\times10^{11}\,\mathrm{m}\right)$. S_{sun} should be normalized to take into account the dependence on the day number n. E_λ is the spectral emissivity, it stands for the spectral power radiated per unit of area and wavelength, its unit is $\mathrm{W\mu m^{-1}m^{-2}}$ [8]. The extra-atmospheric spectral irradiance depends on the earth-sun factor which also depends on the day number [9]. This factor accounts for the change in intensity that occurs as the distance between earth and sun varies during one year [10]. Earth–sun factor is unity when earth-sun distance is at its average value equal to $1\mathrm{A.U}$ as occurs around the 3rd of April and the 1st of October [10]. For a given photon wavelength, I_λ is maximal at perihelion where earth to sun distance is minimal and I_λ is minimal at aphelion where earth to sun distance is maximal (see figure 1) [10].

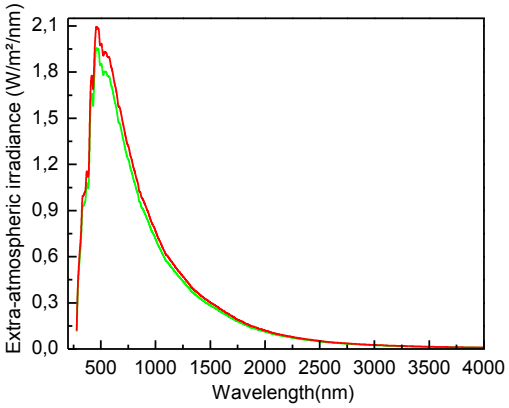

Figure 1. Extra-atmospheric spectral irradiance at perihelion (January the 2nd 2016) (red line) and aphelion (july the 4th 2016) (green line) as a function of photon wavelength.

2.2. The non-uniform daily extra-atmospheric solar "constant"

The extra-atmospheric solar "constant" S_{sun} is the continuous sum i.e. integral of extra-atmospheric spectral irradiance I_λ over the whole electromagnetic spectrum:

$$S_{sun} = \int_0^\infty I_\lambda d\lambda \tag{2}$$

For a given point in the nearest neighbourhood of terrestrial atmosphere, the extra-atmospheric solar ''constant'' S_{sun} depends on the day number *n* as [11]:

$$S_{sun}(n) = 1347.4466\left(1 + 0.034\cos\left(\frac{360(n-2)}{365.25}\frac{\pi}{180}\right)\right) \tag{3}$$

For the leap year 2016, eq. (3) shows that S_{sun} is maximal $\left(1393.25\,\mathrm{Wm^{-2}}\right)$ at perihelion which occurs on January the 2nd, minimal $\left(1301.63\,\mathrm{Wm^{-2}}\right)$ at aphelion which occurs on july the 4th and equal to 1347.44 $\mathrm{Wm^{-2}}$ on April the 2nd (see figure 2). This latter value is obtained by integrating numerically extra-atmospheric spectral irradiance corresponding to april the 2nd between 280 nm and 4000 nm [11]. It's a little bit lighter than 1360.8 $\mathrm{Wm^{-2}}$ which is the most recent value found in the literature [12, 13].

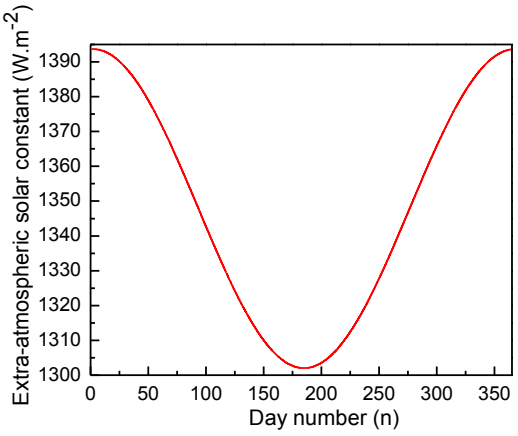

Figure 2. Extra-atmospheric solar constant as a function of the day number n during the leap year 2016.

2.3. The declination of the sun

The declination of the sun $\delta(n)$ is the angle between the ecliptic i.e. the plane containing the earth's orbit and the celestial equator. The declination of the sun $\delta(n)$ depends on the day number n as [14]:

$$\delta(n) = 0.39795\cos\left(\frac{0.98563(n-173)\pi}{180}\right) \tag{4}$$

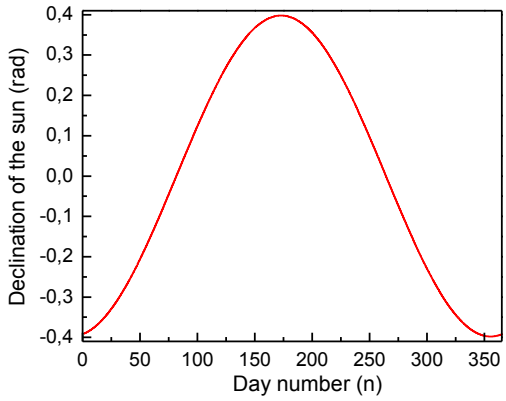

Figure 3. Declination of the Sun i.e. the angle between ecliptic and celestial equator plotted versus day number n during the leap year 2016.

2.4. Horizontal coordinates of the sun

The sun horizontal coordinates according to a given observation site on earth are:

The solar elevation angle or the altitude of the sun. At a given observation site, it's the angle between the centre of the sun's disc and the horizon. It's given by [14]:

$$\sin(h) = \sin(\varphi)\sin(\delta) + \cos(\varphi)\cos(\delta)\cos(\omega) \tag{5}$$

φ is the observation site latitude, δ is the sun declination and ω is the hour angle.

The solar zenith angle θ_z. At a given site, it's the angle between the centre of the sun's disc and the zenith. θ_z is the complementary angle to h, it's expressed as follows [14]:

$$\cos(\theta_z) = \sin(h) \tag{6}$$

The sun azimuth angle a_s, it's the angle between a reference vector pointing towards the north and the perpendicular projection of the sun down onto the horizon. The expression giving a_s is [14]:

$$\sin(a_s) = \frac{\cos(\delta)\sin(\omega)}{\cos(h)} \tag{7}$$

In figure 4, the variations of solar elevation angle h (green line), zenith angle θ_z (red line) and azimuth angle a_s measured in radians clockwise from the north (blue line), are drawn against time during the 346th day of the leap year 2016 for the site of El Jadida (Morocco) (33° 15' 00'' N and 8° 30' 00'' W). One can remark that at sunrise and sunset times, $\theta_z = \pi/2$ and $h = 0$. At solar midday, θ_z is minimal and h is maximal. For the solar azimuth angle, one can notice that it increases monotonically from 2.09 rad at sunrise to 4.22 rad at sunset, passing by π at solar midday.

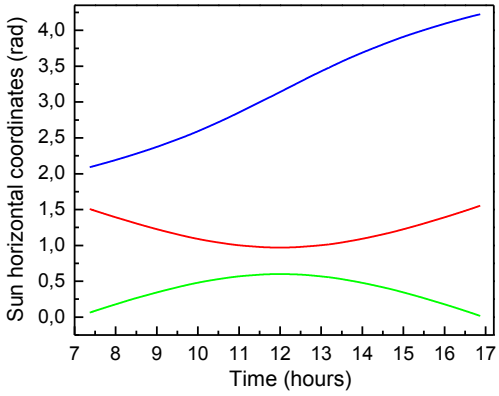

Figure 4. Sun elevation angle (green line), sun zenith angle (red line) and sun azimuth (blue line) at the site of El Jadida (Morocco) plotted against time during the 346th day (December 11th) of the leap year 2016.

2.5. Angle of incidence on a tilted surface

The angle of sunlight incidence on a sloped surface is the angle between sun direction and normal direction to this surface [14]:

$$\cos(\theta) = \cos(\theta_z)\cos(\beta) + \sin(\theta_z)\sin(\beta)\cos(a_s - a) \tag{8}$$

β and a are, respectively, the surface tilt and azimuth angles. For a horizontal surface $\beta = 0$ and $\theta = \theta_z$, for a normal surface to sunlight $\beta = \theta_z$, $a = a_s$ and $\theta = 0$.

2.6. The sunrise and sunset hour angles

In the particular case of a horizontal collector, the sunrise and sunset angles ($-\omega_s$ and ω_s) are obtained by setting $h = 0$ in eq (5) which leads to the following expression:

$$\omega_s(n,\varphi) = \arccos(-\tan(\varphi)\tan(\delta)) \tag{9}$$

In a general case, the tilted collector sunrise and sunset angles (ω_{ss} and ω_{ps}) are solutions of the equation $\theta = \pi/2$ (or $\cos(\theta) = 0$). ω_{ss} and ω_{ps} depend on n, φ, β and a. Taking into account the fact that tilted collector receives sunlight if and only if $-\omega_s \le \omega \le \omega_s$, then the effective tilted collector sunrise and sunset angles are respectively equal to $\max(-\omega_s, \omega_{ss})$ and $\min(\omega_s, \omega_{ps})$.

According to eq (8), one can deduce calculated sunshine duration in hours for a horizontal collector as the difference between times corresponding to sunset and sunrise at a given site:

$$\Delta t_h = \frac{24}{\pi}\arccos(-\tan(\varphi)\tan(\delta)) \tag{10}$$

The calculated sunshine duration in hours for tilted collector at a given site is the difference between times corresponding to effective sunset and sunrise:

$$\Delta t_t = \frac{24}{2\pi}\left(\min(\omega_s, \omega_{ps}) - \max(-\omega_s, \omega_{ss})\right) \tag{11}$$

Figure 5, gives the variations of calculated sunshine duration for horizontal collector (red line) and south-facing tilted collector ($\beta = (33.25)°$, $a = 180°$) (green line) at the site of El Jadida (Morocco) corresponding to the latitude $\varphi = (33.25)°$ as functions of the day number throughout the year.

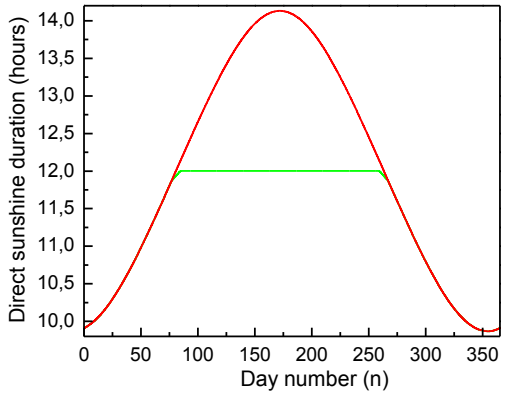

Figure 5. Calculated sunshine duration at the site of El Jadida (Morocco) for horizontal (red line) and tilted (green line) collectors drawn versus day number n during the leap year 2016.

3. Estimated solar irradiance emitted towards the site of El Jadida (Morocco)

3.1. Irradiance emitted towards a tilted surface. Case of a fixed aperture oriented arbitrarily

At a given time *t* in a fixed day *n*, the spectral irradiance $I_\lambda(n)$ is the energy density radiated per unit of time and area in a very short spectral range $d\lambda$. According to eq (2), the irradiance $I(n)$ of the whole spectrum for a fixed day *n* is equal to $S_{sun}(n)$. The elementary energy density per unit of time and area radiated towards a tilted collector, oriented arbitrarily and placed at a given site, during an elementary period of time *dt* corresponding to an elementary rotation of hour angle $d\omega$ such as $d\omega = 2\pi dt/24$, is equal to $S_{sun}(n)\cos(\theta)d\omega$.

The energy density per unit area radiated towards the tilted surface during an entire day is expressed as follows:

$$H_t(n,\varphi,\beta,a) = \frac{24\times 3600}{2\pi}\int_{\max(\omega_{ss},-\omega_s)}^{\min(\omega_{ps},\omega_s)} I(n)\cos(\theta)d\omega \qquad (12)$$

where $\max(-\omega_s,\omega_{ss})$ and $\min(\omega_s,\omega_{ps})$ are respectively effective tilted collector sunrise and sunset angles.

3.2. Irradiance emitted towards a horizontal surface.

The elementary energy density per unit of time and area radiated towards a perpendicular surface to zenith axis placed at a given site during an elementary rotation of hour angle $d\omega$ is equal to $S_{sun}(n)\cos(\theta_z)\,d\omega$.

The energy density radiated per unit area towards a perpendicular surface to zenith axis during one day is expressed as follows:

$$H_h(n,\varphi) = \frac{24\times 3600}{2\pi}\int_{-\omega_s}^{\omega_s} I(n)\left(\sin(\varphi)\sin(\delta)+\cos(\varphi)\cos(\delta)\cos(\omega)\right)d\omega \qquad (13)$$

where $-\omega_s$ and ω_s are respectively horizontal collector sunrise and sunset angles.

3.3. Irradiance emitted towards a perpendicular surface to incident radiation. Case of a two-axis tracking aperture

The energy density per unit area radiated towards a perpendicular surface to incident radiation placed at a given extra-atmospheric observation site during one day reads as follows:

$$H_p(n,\varphi) = \frac{24\times 3600}{2\pi}\int_{-\omega_s}^{\omega_s} I(n)\, d\omega \tag{14}$$

3.4. Irradiance emitted towards a tilted surface. Case of a single-axis tracking aperture
When the tracking axis is oriented in north to south direction, eq (8) reduces to [14]:

$$\cos(\theta) = \sqrt{1-\left(\sin(\varphi)\sin(\delta)+\cos(\varphi)\cos(\delta)\cos(\omega)\right)^2} \tag{15}$$

The energy density per unit area radiated towards this mobile tilted surface during one day writes as follows:

$$H_{s-a,n-s}(n,\varphi) = \frac{24\times 3600}{2\pi}\int_{-\omega_s}^{\omega_s} I(n)\sqrt{1-\left(\sin(\varphi)\sin(\delta)+\cos(\varphi)\cos(\delta)\cos(\omega)\right)^2}\, d\omega \tag{16}$$

When the tracking axis is oriented in east to west direction, eq (8) reduces to [14]:

$$\cos(\theta) = \sqrt{1-\left(\cos(\delta)\sin(\omega)\right)^2} \tag{17}$$

The energy density per unit area emitted towards this mobile sloped surface during one day writes as follows:

$$H_{s-a,e-w}(n,\varphi) = \frac{24\times 3600}{2\pi}\int_{-\omega_s}^{\omega_s} I(n)\sqrt{1-\left(\cos(\delta)\sin(\omega)\right)^2}\, d\omega \tag{18}$$

3.5. Annual irradiance mean value
In the particular case where the sun inclination is considered as constant during the day, the annual mean value of energy density per unit area $H_i(\varphi,\beta,a)$ for a given observation site writes:

$$\langle H_i\rangle(\varphi,\beta,a) = \frac{1}{366}\sum_{n=1}^{366} H_{i,n}(\varphi,\beta,a) \tag{19.1}$$

In all cases, the annual mean value of energy density per unit area $H_i(n,\varphi,\beta,a)$ for a given observation site writes:

$$\langle H_i\rangle(\varphi,\beta,a) = \frac{1}{365.25}\int_0^{365.25} H_i(n,\varphi,\beta,a)\, dn \tag{19.2}$$

where i is identified with *t, h, p, (s-a, n-s)* and *(s-a, e-w)* respectively for tilted, horizontal, perpendicular, single-axis oriented in east-west direction and single-axis oriented in north-south direction collectors.

In sections 3.1 to 3.5, Maple computer algebra software is used to derive analytic expressions for ω_{ss} and ω_{ps} and to achieve symbolic and numeric calculation of $H_i(n,\varphi,\beta,a)$ and $\langle H_i\rangle(\varphi,\beta,a)$. Due to excessive lengths of analytic expressions of $H_i(n,\varphi,\beta,a)$, we simply present their variations as functions of the day number *n*.

In figure 6, daily energy densities (solar radiation or solar insolation) radiated towards horizontal collector (red line), south-facing fixed tilted collector ($\beta = (33.25)°$, $a = 180°$) (green line), north-south direction oriented single-axis collector (cyan line), east-west direction oriented single-axis collector (magenta line) and perpendicular collector to sunlight (blue line) are drawn as functions of the day number n for the observation site of El Jadida (Morocco). Dashed lines correspond to annual mean values of energy densities.

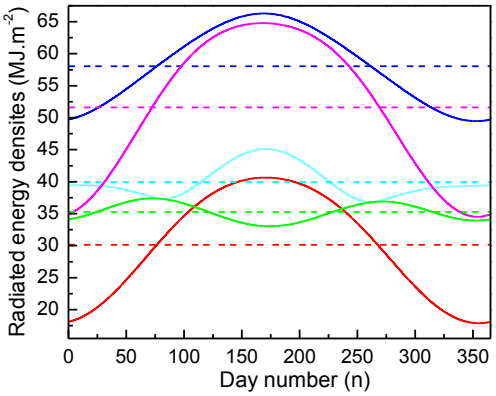

Figure 6. Daily energy densities (solid lines) and annual mean values of energy densities (dashed lines) radiated towards horizontal (red line), south facing fixed tilted (green line) north-south direction oriented single-axis (cyan line) east-west direction oriented single-axis (magenta line) and perpendicular (blue line) collectors at the site of El Jadida (Morocco) plotted versus the day number n.

4. Experimental measures of daily irradiance received at the site of El Jadida (Morocco)

4.1. Tracking global irradiance received by fixed tilted and horizontal collectors at the site of El Jadida

In the present work, we use two datasets of experimental values coming from two stations. The first dataset gathers experimental values collected during two years by A Rerhrhaye and M S El Maliki [7, 15, 16] in the Solar Energy Laboratory which is equipped with two Kipp and Zonen CM11 pyranometers. The first pyranometer measures the global horizontal irradiation. The second pyranometer, equipped with a sunscreen band, measures horizontal diffuse irradiation. These two instruments are linked to a Kipp and Zonen CC12 solar integrator which records the hourly values of these two quantities. The duration of insolation is measured by a Campelle-Stockes heliograph. The experimental setup allows tracking of global horizontal irradiance and diffuse horizontal irradiance every five minutes. The second dataset gathers experimental values corresponding to twelve days. They are collected by M Khaidar and L Birba [15, 17, 18] in Condensed Matter Laboratory which is equipped with two photovoltaic receivers allowing indirect measurement of horizontal and tilted irradiances from the output power. The first photovoltaic receiver is horizontal, the second one is south facing and tilted with an inclination angle equal to the latitude of El Jadida. This experimental setup allows tracking of global horizontal and tilted irradiances every five minutes. To achieve a comparison between estimates based on numerical and symbolic calculations performed in section 3, and energy density effectively received on the earth, we proceed to a careful analysis of experimental global irradiance received by tilted and horizontal apertures from metrological and photovoltaic stations at El Jadida University (Morocco). We also use simulated values of direct, diffuse and global irradiances from Climate-SAE PVGIS databank [19, 20].

4.2. The Concept of Air Mass (AM)

The Air Mass coefficient (AM) is the direct optical path length through earth's atmosphere to zenith optical path length ratio. In this paper, we work with the most accurate model of Air Mass which considers the earth as a sphere and the atmosphere as a spherical layer around it:

$$AM(\theta_z) = \sqrt{\left(\left(r\cos\left(\theta_z\right)\right)^2 + 2r + 1\right)} - r\cos\left(\theta_z\right) \tag{20}$$

where $r = 796$ is the earth's radius to atmosphere thickness ratio [21].

4.3. Modelling direct normal, diffuse horizontal and global irradiances

The solar radiation reaching a horizontal collector on earth is composed by direct horizontal component B_h and diffuse horizontal component D_h. The sum of these components makes the global radiation: $G_h = B_h + D_h$.

Taking into account atmospheric absorption depicted by the concept of Air Mass, direct normal irradiance may be described by the following model:

$$B_n = I(n)\left(A + B\exp\left(-C\left(AM(\theta_z)\right)\right)\right) \quad (21)$$

The direct horizontal irradiance B_h and direct tilted irradiance B_t may be deduced from eq (21) by: $B_h = B_n \cos(\theta_z)$ and $B_t = B_n \cos(\theta)$.

The diffuse horizontal component D_h may be depicted by the following model:

$$D_h = I(n)\cos(\theta_z)\left(D + EB\left(1 - \exp\left(-CAM(\theta_z)\right)\right)\right) \quad (22)$$

Concerning diffuse tilted irradiance, it may be found by applying Liu and Jordan equation [22]: $D_t = D_h(1+\cos(\beta))/2$.

The global horizontal irradiance G_h collected locally is then modelled by the following equation:

$$G_h = I(n)\cos(\theta_z)\left(A + D + EB + B(1-E)\left(\exp\left(-CAM(\theta_z)\right)\right)\right) \quad (23)$$

The models proposed of direct normal irradiance eq (21), diffuse horizontal irradiance eq (22) and global horizontal irradiance eq (23) are different from other models in the literature [23, 24]. *A*, *B*, *C*, *D* and *E* are real parameters which are varied numerically to fit simulated data from PVGIS and experimental data from local station to models of eq (21), (22) and (23) by minimizing the sum of squared errors. These parameters are determined for twelve average days of the year i.e. one average day for each month. In tables 1 and 2, we respectively give parameters values corresponding to the models fitting well with data from Climate-SAE PVGIS and experimental irradiance measured at the site of El Jadida [15, 17, 18].

Table 1. Numerical values of parameters corresponding to models fitting well with data from Climate-SAE PVGIS for twelve average days of the year.

Date	A (Wm^{-2})		B (Wm^{-2})		C		D (Wm^{-2})		E	
	PVGIS normal sky	PVGIS clear sky	PVGIS normal sky	PVGIS clear sky	PVGIS normal sky	PVGIS clear sky	PVGIS normal sky	PVGIS clear sky	PVGIS normal sky	PVGIS clear sky
10 Jan	0.115	0.156	0.499	0.677	0.212	0.212	0.087	0.062	0.580	0.304
15 Feb	0.109	0.140	0.552	0.711	0.268	0.269	0.080	0.062	0.508	0.303
16 Mar	0.130	0.180	0.479	0.709	0.247	0.199	0.090	0.035	0.870	0.310
15 Apr	0.151	0.187	0.575	0.712	0.349	0.349	0.045	0.032	0.590	0.355
16May	0.205	0.260	0.540	0.682	0.408	0.409	0.024	0.013	0.644	0.355
16 Jun	0.215	0.263	0.558	0.685	0.441	0.441	0.018	0.013	0.615	0.356
17 Jul	0.199	0.219	0.646	0.712	0.460	0.460	0.024	0.020	0.478	0.366
16Aug	0.166	0.178	0.671	0.725	0.412	0.410	0.038	0.035	0.434	0.355
16 Sep	0.140	0.163	0.619	0.721	0.341	0.341	0.055	0.044	0.490	0.339
16 Oct	0.136	0.162	0.595	0.707	0.317	0.318	0.072	0.055	0.482	0.322
15 Nev	0.111	0.144	0.545	0.701	0.249	0.249	0.083	0.067	0.467	0.280
11 Dec	0.116	0.172	0.463	0.688	0.181	0.181	0.088	0.052	0.610	0.249

Table 2. Numerical values of parameters corresponding to models fitting well with experimental measures for twelve average days of the year.

Date	A (Wm^{-2})	B (Wm^{-2})	C	D (Wm^{-2})	E
10 Jan	0.063	0.792	0.249	0.077	0.177
15 Feb	0.120	0.586	0.328	0.239	0.153
16 Mar	0.167	0.643	0.220	0.084	0.090
15 Apr	0.064	0.875	0.294	0.021	0.115
16 May	0.071	0.878	0.442	0.128	0.011
16 Jun	0.123	0.783	0.401	0.107	0.010
17 Jul	0.153	0.692	0.285	0.030	0.011
16Aug	0.120	0.822	0.526	0.011	0.103
16 Sep	0.089	0.737	0.475	0.021	0.010
16 Oct	0.112	0.701	0.203	0.089	0.077
15 Nev	0.143	0.715	0.263	0.095	0.069
11 Dec	0.050	0.830	0.288	0.027	0.167

In this study, we define clear and normal states of the sky as the situations for which diffuse transmission function at the zenith is respectively equal to 0.05 and 0.22 [7].

In figure 7, the variations of direct normal irradiance B_n values from PVGIS databank (dashed lines) and their numerical models (solid lines) for clear (red lines) and normal (green lines) skies are plotted as functions of time during december 11th 2016. As expected, B_n vanishes for sunrise and sunset times and is maximal for solar midday. In addition, one can remark that the model proposed in eq (21) fits perfectly with simulated data from PVGIS.

In figure 8, variations of diffuse horizontal irradiance D_h values from PVGIS databank (dashed lines) as well as its numerical models (solid lines) for clear (red lines) and normal (green lines) skies are drawn versus time throughout december 11th 2016. Here also, one can easily notice that the model proposed in eq (22) gives a good description of diffuse horizontal irradiance in a clear contrast with some models given in the litterature [25, 26].

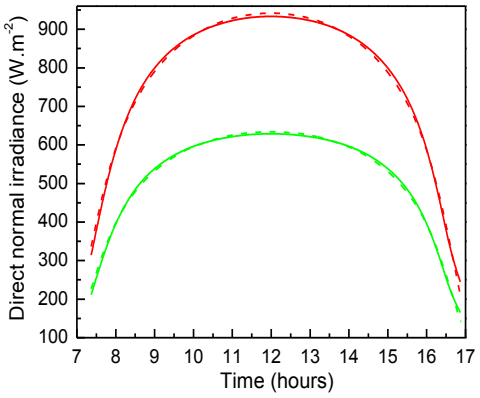

Figure 7. Direct normal irradiance B_n data from Climate-SAE PVGIS (dashed lines) and its numerical models (solid lines) for clear (red lines) and normal (green lines) skies drawn against time during December 11th 2016.

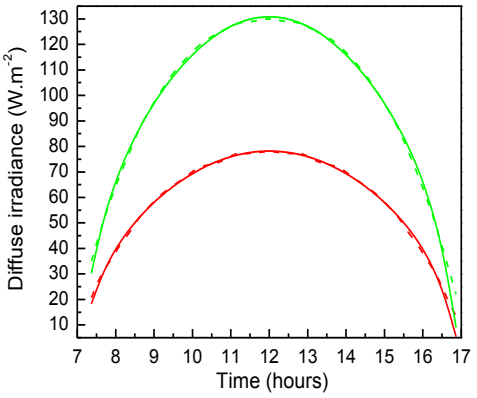

Figure 8. Diffuse horizontal irradiance D_h values from Climate-SAE PVGIS (dashed lines) and its numerical models (solid lines) for clear (red lines) and normal (green lines) skies drawn against time during December 11th 2016.

Figure 9 presents experimental measurements collected locally and simulated values from PVGIS databank of global irradiance G_h (dashed lines) at El Jadida (Morocco) as well as their numerical models

(solid lines) for clear (red lines) and normal (green lines) skies as functions of time during december 11th 2016. Blue lines correspond to experimental data and its numerical model. We can remark that experimental measurements are lying between clear and normal skies data, we also notice that maximal value of D_h reaches $138.82\,\mathrm{Wm^{-2}}$ at midday which is consistent with cloudy days of December.

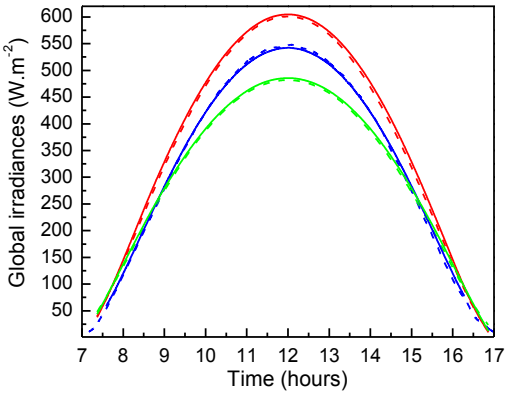

Figure 9. Experimental measurements and simulated values from Climate-SAE PVGIS of global irradiance G_h (dashed lines) and their numerical models (solid lines) for clear (red lines) and normal (green lines) skies plotted versus time during December 11th 2016. Experimental data correspond to blue lines.

4.4. Prediction of daily energy density received at the site of El Jadida (Morocco):
The daily energy density received at the site of El Jadida (Morocco) by an arbitrarily oriented surface during one day is expressed as follows:

$$H_i(n,\beta,a) = 3600\sum_{j=1}^{N}\left(G_{i,j+1}(n,\beta,a) + G_{i,j}(n,\beta,a)\right)\frac{\left(t_{j+1}-t_j\right)}{2} \tag{24}$$

where i is identified with *t*, *h*, *p*, *(s-a, n-s)* and *(s-a, e-w)* respectively for tilted, horizontal, perpendicular, single-axis oriented in east-west direction and single-axis oriented in north-south direction collectors.
In table 3, the values of incident and received energy per unit area for horizontal, normal and tilted fixed surfaces with $\beta = (33.25)°$ and $a = 180°$ for the average day of December 2016 are gathered.

Table 3. Daily energy densities radiated and received at El Jadida (Morocco) by horizontal, normal and tilted fixed apertures ($\beta = (33.25)°$, $a = 180°$).

n = 346	Daily energy densities radiated and received at El Jadida (Morocco) ($\mathrm{MJm^{-2}}$)		
	Horizontal aperture	Two-axis aperture	Tilted fixed aperture
Radiated extra-atmospheric	18.06	49.57	34.00
Global for clear sky	13.16	28.89	22.10
Global for normal sky	10.91	20.73	16.62
Global experimental	11.56	-	20.58

As mentioned above, the values of models parameters are determined for 12 average days, one average day for each month, from experimental measurements and simulated data from PVGIS. Then, numerical interpolations are performed to generate the values of models parameters for each day of the year and to calculate daily direct, diffuse and global irradiances using the equation:

$$H_i(n,\varphi,\beta,a)=\frac{24\times 3600}{2\pi}\int_{\max(\omega_{ss},-\omega_s)}^{\min(\omega_{ps},\omega_s)} G_i(n)d\omega \tag{25}$$

where G_i is collector global irradiance given in paragraph 4.3 which is dependent on interpolated values of *A*, *B*, *C*, *D* and *E* for normal sky. i is identified with *t*, *h* and *p*, respectively for tilted, horizontal and perpendicular to sun rays apertures. This allows us to predict, with a good degree of accuracy, energy densities received by horizontal, normal and fixed tilted apertures (see figure 10).

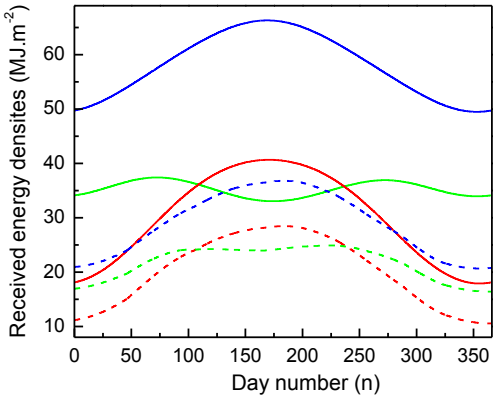

Figure 10. Calculated daily energy densities radiated (solid lines) and effectively received (dashed lines) by normal to sun rays (blue lines), horizontal (red lines) and fixed tilted apertures with $\beta=(33.25)°$, $a=180°$ (green lines) as functions of the day number.

In figure 11, we present daily energy densities measured locally and calculated according eq (25) and using the model given in paragraph 4.3 for a horizontal collector at the site of El Jadida. The reader can notice that measured and calculated data are in good agreement.

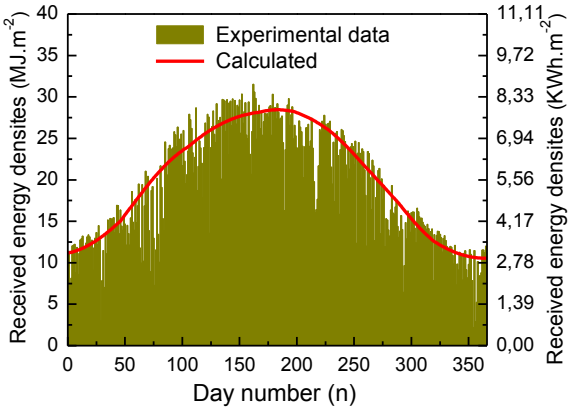

Figure 11. Daily energy densities measured and calculated for a horizontal collector at the site of El Jadida as functions of the day number n.

5. Conclusion

In this paper, Maple computer algebra software is used to determine analytic expressions and to calculate numerical values of daily solar radiation directed towards horizontal, fixed tilted, single-axis and double-axis tracking collectors placed outside atmosphere as functions of the day number, collector latitude, collector tilt and azimuth angles. Effects of non-uniform atmospheric absorption of incident solar radiation throughout a day, from sunrise to sunset, are taken into account and new models of direct normal and diffuse horizontal components of daily global horizontal and tilted irradiances are proposed, tested and validated on local experimental data. This enables us to extract global irradiance model parameters for average day of each month and to predict, accurately, daily solar radiation (energy per unit area) effectively received by any collector placed on earth during the whole year.

Acknowledgments
The authors H El Achouby and M Zaimi are grateful to Kingdom of Morocco Ministry of Higher Education and to Chouaïb Doukkali University for their financial supports.

References
[1] http://data.worldbank.org/topic/energy-and-mining
[2] http://data.worldbank.org/topic/climate-change
[3] Loi 13-09 relative aux énergies renouvelables March 18th 2010 *Bulletin Officiel du Royaume du Maroc* N° 5822 pp 229
[4] Loi 16-09 relative à l'Agence Nationale pour le Développement des Energies Renouvelables et de l'Efficacité Energétiques March 18th 2010 *Bulletin Officiel du Royaume du Maroc* N° 5822, pp 235
[5] Loi 57-09 portant création de la société ''Moroccan Agency for Solar Energy'' March 18th 2010 *Bulletin Officiel du Royaume du Maroc* N° 5822 pp 237
[6] http://noorouarzazate.com/
[7] Rerhrhaye A 1995 Caractérisation du gisement solaire du site d'El Jadida Thèse de Doctorat d'Etat en Physique Université Chouaïb Doukkali Faculté des Sciences (El Jadida)
[8] Castaner L and Silvestre S 2002 Modelling Photovoltaic Systems Using PSpice *John Wiley and Sons* (Chichester, England)
[9] Gueymard C 2004 The sun's total and spectral irradiance for solar energy applications and solar radiation models *Solar Energy* **76** (2004) 423–453
[10] https://www.pvlighthouse.com.au
[11] Gueymard C 1995 SMARTS2, A simple model of the atmospheric radiative transfer of sunshine: Algorithms and performance assessment *Florida Solar Energy Center*
[12] Sengupta M, Habte A, Gueymard C, Wilbert S and Renné D 2017 Best Practices Handbook for the Collection and Use of Solar Resource Data for Solar Energy Applications: Second Edition NREL Technical Report http:/www.osti.gov/scitech
[13] Kopp G and Lean J L 2011 A new lower value of total solar irradiance: evidence and climate significance Geophys Res Lett **38**:L01706
[14] William B S and Michael G 2001 Power From The Sun http://www.powerfromthesun.net/book.html
[15] El Maliki M S 2017 Modèles d'estimation des composantes du rayonnement solaire & Productivité photovoltaïque d'installations connectées au réseau Habilitation Universitaire en Energétique Université Chouaïb Doukkali Faculté des Sciences (El Jadida)
[16] Rerhrhaye A, El Maliki M S and Zehaf M 2002 Estimation des valeurs quotidiennes du diffus sur surface horizontale Phys. Chem. News **6** 18-22
[17] Birba L, Khaidar M, Zradba A, Monkade M, El Maliki M S, Zehaf M, Rerhrhaye A, Aarich N, Raoufi M and Bennouna A 2016 The behaviour of a grid connected PV plant under a semiarid and maritime climates in summer 1st International Conference on Solar Energy and Materials (Marrakesh)
[18] Birba L, Khaidar M, Louardi A, Monkade M, Zradba A, El Maliki M S and Zehaf M 2017 Modeling of photovoltaic systems taking into account the thermal inertia of PV materials The International conference on Advanced Materials for Photonics, Sensing and Energy Applications (Agadir)
[19] Suri M, Huld T and Dunlop E 2005 PVGIS, a Web Based Solar Radiation Database for the Calculation of PV Potential in Europe *Int. J. of Sustainable Energy* **24** (2) 55-67
[20] http://re.jrc.ec.europa.eu/pvgis/apps4/pvest.php?map=africa&lang=fr
[21] Bruneton E and Neyret F 2008 Precomputed atmospheric scattering *Comput. Graph. Forum*. **27** (4) Special Issue: Proceedings of the 19th Eurographics Symposium on Rendering 1079–1086
[22] Liu B Y H and Jordan R C 1961 Daily insolation on surfaces tilted towards the equator *ASHRAE Journal* **3** (0) 53–59
[23] El Mghouchi Y, El Bouardi A, Choulli Z and Ajzoul T 2016 Models for obtaining the daily direct, diffuse and global solar radiations Renewable and Sustainable Energy Reviews **56** 87-99

[24] El Mghouchi Y, Ajzoul T and El Bouardi A 2016 Prediction of daily solar radiation intensity by day of the year in twenty-four cities of Morocco Renewable and Sustainable Energy Reviews **53** 823-831
[25] Perrin de Brichambaut C 1975 Estimation des Ressources Energétiques en France *Cahiers de l'A. FEDES, N°1*
[26] Capderou M 1985 Editor of Atlas solaire de l'Algérie énergétique Tome 2. **2** 140–399 (Alger)